RESEARCH ARTICLE SUMMARY

IMMUNE SIGNALING

Nuclear hnRNPA2B1 initiates and amplifies the innate immune response to DNA viruses

Lei Wang*, Mingyue Wen*, Xuetao Cao†

INTRODUCTION: Recognition of pathogen-derived nucleic acids by host cells is an evolutionarily conserved mechanism that induces immune defense responses to microbial infections. Most DNA viruses direct their genomic DNA into host cell nuclei, which can serve as an important molecular signature of DNA virus infection. However, little is known about the nuclear surveillance mechanisms for viral nucleic acids.

RATIONALE: Virus-induced type I interferon (IFN-I) expression depends on the TANK-binding kinase 1–interferon regulatory factor 3 (TBK1–IRF3) activation. We reasoned that nuclear DNA sensors may translocate to the cytoplasm to activate the TBK1–IRF3 pathway after recognizing viral DNA in the nucleus. Thus, we screened nuclear proteins that bound viral DNA and translocated from the nucleus to the cytoplasm after viral infection. Heterogeneous nuclear ribonucleoprotein A2B1 (hnRNPA2B1) was identified as a potential DNA sensor. We then conducted a series of in vivo and in vitro experiments to probe the biological importance and activation mechanisms of hnRNPA2B1. Additionally, we explored its relationship with known cytosolic stimulator of interferon genes (STING)–dependent DNA sensors such as cyclic GAMP synthase (cGAS).

RESULTS: hnRNPA2B1 was found to bind viral DNA in the cell nucleus during herpes simplex virus–1 (HSV-1) infection. It then translocated to the cytoplasm and activated TBK1 through the tyrosine kinase Src. Accordingly, hnRNPA2B1 knockdowns and deficiency resulted in impaired DNA virus– but not RNA virus–induced IFN-I production and prolonged viral replication. The production of proinflammatory cytokines such as tumor necrosis factor–α (TNF-α) and interleukin-6 (IL-6) was unaffected. hnRNPA2B1 became dimerized after HSV-1 infection. Mutation of the dimer interface abrogated its nucleocytoplasmic translocation upon HSV-1 infection. Thus, hnRNPA2B1 dimerization is required for its nucleocytoplasmic translocation. Additionally, hnRNPA2B1 was demethylated at Arg^{226} after HSV-1 infection, which led to its activation and the subsequent initiation of IFN-β expression. This demethylation was catalyzed by the arginine demethylase JMJD6. hnRNPA2B1 with dimer interface mutation was unable to associate with JMJD6 after HSV-1 infection and showed increased amounts of arginine methylation compared to full-length hnRNPA2B1, indicating that dimerization was required for its demethylation.

ON OUR WEBSITE

Read the full article at http://dx.doi.org/10.1126/science.aav0758

To probe the relationship between hnRNPA2B1 and the recognized DNA sensor pathways, we found that the overexpression of hnRNPA2B1 increased HSV-1–induced TBK1 activation and *Ifnb1* expression in $Cgas^{-/-}$ L929 cells. Thus, hnRNPA2B1 could induce IFN-I in a cGAS-independent manner at least in part. This is consistent with earlier evidence suggesting the existence of other IFN-I–initiating molecules in the innate response against DNA virus. Wild-type macrophages showed higher and more sustained *Ifnb1* expression than $Hnrnpa2b1^{-/-}$ macrophages in response to DNA viruses. Thus, hnRNPA2B1 was required for fully activating type I interferon production against DNA viruses mediated by cGAS, interferon-γ–inducible protein 16 (IFI16), and STING pathways. Mechanistically, hnRNPA2B1 bound *CGAS*, *IFI16*, and *STING* mRNAs and promoted their nucleocytoplasmic trafficking to amplify cytoplasmic innate sensor signaling. The translation of these mRNAs was impaired in the absence of hnRNPA2B1 after HSV-1 infection. hnRNPA2B1 was constitutively associated with fat mass and obesity-associated protein (FTO). This association was abrogated after HSV-1 infection. By this means, hnRNPA2B1 promoted the N^6-methyladenosine (m^6A) modification and nucleocytoplasmic trafficking of *CGAS*, *IFI16*, and *STING* mRNAs. Thus, hnRNPA2B1 facilitates the efficient induction of antiviral IFN-I production mediated by cGAS, IFI16, and STING.

CONCLUSION: We identified hnRNPA2B1 as an innate sensor that initiates type I IFN production upon DNA virus infection in the nucleus. hnRNPA2B1 also amplifies type I IFN responses by directly enhancing STING-dependent cytosolic DNA sensing pathways. ■

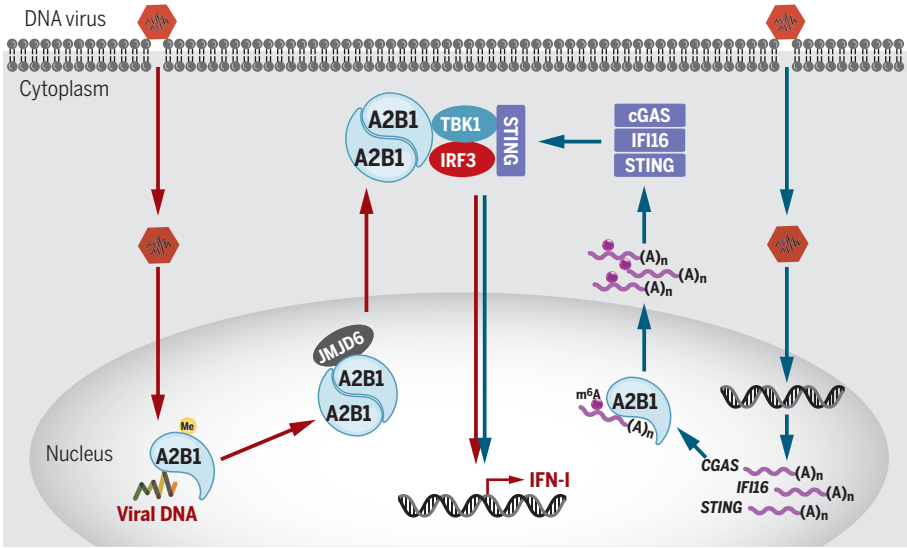

hnRNPA2B1 senses viral DNA in the nucleus and then activates and amplifies type I IFN responses. Upon entry, viral DNA is mainly enveloped within capsids. After traversing to the nucleus, DNA viruses eject their genomic DNA into the nucleus, which is recognized by hnRNPA2B1. Upon recognition of viral DNA, hnRNPA2B1 forms a homodimer, which is then demethylated by JMJD6. It consequently translocates to the cytoplasm where it activates the TBK1–IRF3 pathway and initiates IFN-α/β production. Additionally, hnRNPA2B1 promotes m^6A modification, nucleocytoplasmic trafficking, and translation of *CGAS*, *IFI16*, and *STING* mRNAs to fully ensure the activation of IFN-α/β in response to DNA virus infection.

The list of author affiliations is available in the full article online.
*These authors contributed equally to this work.
†Corresponding author. Email: caoxt@immunol.org
Cite this article as L. Wang *et al.*, *Science* **365**, eaav0758 (2019). DOI: 10.1126/science.aav0758

RESEARCH ARTICLE

IMMUNE SIGNALING

Nuclear hnRNPA2B1 initiates and amplifies the innate immune response to DNA viruses

Lei Wang[1,2]*, Mingyue Wen[2]*, Xuetao Cao[1,2,3]†

DNA viruses typically eject genomic DNA into the nuclei of host cells after entry. It is unclear, however, how nuclear pathogen–derived DNA triggers innate immune responses. We report that heterogeneous nuclear ribonucleoprotein A2B1 (hnRNPA2B1) recognizes pathogenic DNA and amplifies interferon-α/β (IFN-α/β) production. Upon DNA virus infection, nuclear-localized hnRNPA2B1 senses viral DNA, homodimerizes, and is then demethylated at arginine-226 by the arginine demethylase JMJD6. This results in hnRNPA2B1 translocation to the cytoplasm where it activates the TANK-binding kinase 1–interferon regulatory factor 3 (TBK1–IRF3) pathway, leading to IFN-α/β production. Additionally, hnRNPA2B1 facilitates N^6-methyladenosine (m^6A) modification and nucleocytoplasmic trafficking of *CGAS*, *IFI16*, and *STING* messenger RNAs. This, in turn, amplifies the activation of cytoplasmic TBK1–IRF3 mediated by these factors. Thus, hnRNPA2B1 plays important roles in initiating IFN-α/β production and enhancing stimulator of interferon genes (STING)–dependent cytoplasmic antiviral signaling.

Host innate immune responses to viruses can be triggered by the recognition of viral nucleic acids through pattern recognition receptors (PRRs). This results in the production of proinflammatory cytokines regulated by nuclear factor κB (NF-κB) signaling and type I interferons mediated by interferon regulatory factor (IRF) signaling (*1*, *2*). Typically, once DNA viruses enter a host cell, they eject and replicate their genomic DNA within host cell nuclei (*3*). The process by which pathogen-derived DNA is recognized within the nucleus remains an enigma, however. To date, only one protein, interferon-γ–inducible protein 16 (IFI16), has been proposed to recognize DNA viruses within the nucleus and activate type I interferon (IFN-I) production and inflammasome responses (*4*, *5*). Given how frequently host cells encounter nuclear pathogen–derived DNA, we therefore sought to identify other uncharacterized IFN-I initiators within the nucleus.

Many proteins that can recognize viral DNA and induce IFN-α/β production have been identified (*6*), such as RNA polymerase III, IFI16, DNA-dependent activator of interferon regulatory factors (DAI), leucine-rich repeat flightless-interacting protein 1 (LRRFIP1), LSm14A, meiotic recombination 11 homolog A (MRE11), heterotrimeric protein complex DNA-PK, high-mobility group box proteins (HMGBs), DExD/H helicase DDX41, and cyclic GMP-AMP (cGAMP) synthase (cGAS) (*7*–*16*). Nevertheless, only cytoplasmic cGAS and DNA-PK have been functionally validated as DNA sensors in vivo (*8*, *17*). Several proteins have also been reported to be involved in the DNA virus-induced inflammatory response, including absent in melanoma 2 (AIM2), IFI16, Rad50, and Sox2 (*4*, *18*–*20*). Thus, a fuller understanding of innate immune responses against DNA viruses is needed, especially regarding pathways that link the nuclear recognition of pathogen-derived DNA with the activation of cytoplasmic signaling.

We examined the nuclear proteins that bind to the genomic DNA of herpes simplex virus–1 (HSV-1) as well as translocate to the cytoplasm after viral infection. This analysis uncovered heterogeneous nuclear ribonucleoprotein A2B1 (hnRNPA2B1) as a nuclear initiator of type I interferon production that restricts DNA virus infection. After directly recognizing nuclear pathogen–derived DNA, hnRNPA2B1 translocates to the cytoplasm to initiate innate immune responses. hnRNPA2B1 then simultaneously facilitates the nucleocytoplasmic translocation and cytoplasmic expression of mRNAs such as *CGAS*, *IFI16*, and *STING* mRNA, which amplify antiviral innate immune signaling.

Results

Identification of hnRNPA2B1 as a candidate DNA sensor for type I IFN production

To identify potential nuclear DNA sensors, we biotinylated the genomic DNA of HSV-1 (F strain), precipitated the DNA-bound proteins from nuclear extracts of RAW264.7 cells, and examined the proteins that might bind HSV-1 genomic DNA by mass spectrometry (MS) (fig. S1A). Additionally, we separated the nuclear and cytoplasmic proteins after HSV-1 infection by two-dimensional (2D) SDS–polyacrylamide gel electrophoresis (SDS-PAGE), and then subjected those proteins that translocated from the nucleus to the cytoplasm 2 hours after HSV-1 infection to MS assays (fig. S1B). By integrating these two approaches, we identified 23 potential pathogen-derived DNA-binding proteins (table S1). Preliminary small interfering RNA (siRNA)–based functional screening pointed to one candidate in particular, hnRNPA2B1, as a putative IFN-I–inducing nuclear sensor. The interaction of hnRNPA2B1 with biotinylated HSV-1 DNA could be blocked competitively by unlabeled HSV-1 DNA (Fig. 1A). Human and mouse DNA also competitively blocked the binding of hnRNPA2B1 to biotinylated HSV-1 DNA. By contrast, human native nucleosomes, where genomic DNA wraps around a protein complex, could not (Fig. 1B). Thus, hnRNPA2B1 binds both self- and pathogen-derived DNA. Furthermore, chromosomal proteins block the binding of hnRNPA2B1 to self-DNA. HSV-1 DNA was precipitated through hnRNPA2B1 immunoprecipitation after HSV-1 infection, further suggesting that hnRNPA2B1 binds HSV-1 DNA during infection (Fig. 1C).

Heterogeneous nuclear ribonucleoproteins (hnRNPs) comprise a family of at least 20 abundant proteins and other less-abundant proteins in human cells. These RNA-binding proteins (RBPs) are involved in mRNA splicing, transport, and other mRNA and microRNA (miRNA) events (*21*). hnRNPA2B1 contains two tandem RNA/DNA-recognition motifs (RRMs) at the N terminus (fig. S1C), suggested to have DNA-binding capacity (*22*). Mutants lacking RRMs failed to bind biotinylated HSV-1 DNA (fig. S1D), indicating that the RRMs of hnRNPA2B1 mediate its recognition of HSV-1 DNA.

To delineate the potential roles of hnRNPA2B1 in initiating IFN-I production, we silenced hnRNPA2B1 in various mouse macrophage populations, including RAW264.7 cells, primary peritoneal macrophages (PMs), and bone marrow–derived macrophages (BMDMs) (fig. S2A). This significantly impaired HSV-1–induced mRNA expression and protein production of IFN-α, IFN-β, and CXCL10, but not interleukin-6 (IL-6) and tumor necrosis factor–α (TNF-α) (fig. S2, B to H). Thus, hnRNPA2B1 appears to play a role in DNA virus–induced IFN-I production. Knockdown of hnRNPA2B1 in PMs and BMDMS had no effect on IFN-β expression induced by RNA virus [vesicular stomatitis virus (VSV) and Sendai virus (SeV)] infections (fig. S2, I and J). A second siRNA was used to exclude off-target effects, and similar results were obtained (fig. S2, K and L). Furthermore, knockdown of hnRNPA2B1 in THP-1 cells significantly impaired HSV-1–induced but not VSV-induced *IFNA4*, *IFNB1*, *CCL5*, and *CXCL10* expression. However, *IL6* and *TNFA*

[1]National Key Laboratory of Medicinal Chemical Biology, College of Life Science, Nankai University, Tianjin 300071, China. [2]National Key Laboratory of Medical Immunology and Institute of Immunology, Second Military Medical University, Shanghai 200433, China. [3]National Key Laboratory of Medical Molecular Biology and Department of Immunology, Institute of Basic Medical Sciences, Peking Union Medical College, Chinese Academy of Medical Sciences, Beijing 100005, China.
*These authors contributed equally to this work.
†Corresponding author. Email: caoxt@immunol.org

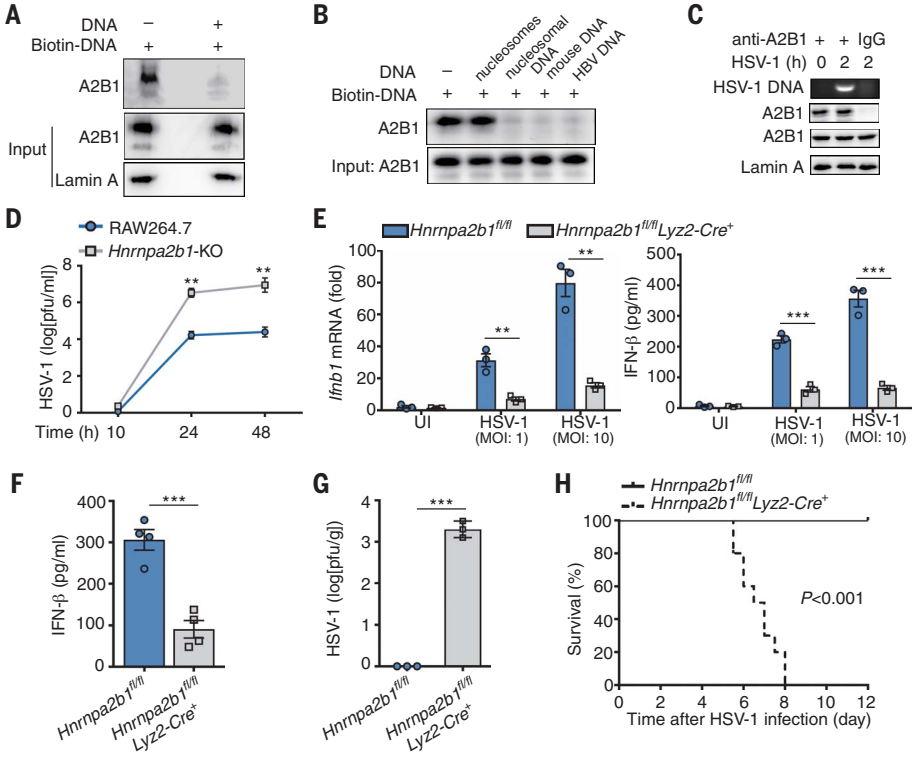

Fig. 1. hnRNPA2B1 activates antiviral defense to inhibit DNA virus replication. (**A**) Complexes obtained by nucleic acid affinity purification were examined by immunoblot in the absence or presence of unlabeled HSV-1 DNA using antibodies against hnRNPA2B1 (anti-hnRNPA2B1). (**B**) hnRNPA2B1 was pulled down and then incubated with unlabeled human native nucleosome, human nucleosomal DNA, mouse DNA, or HBV DNA. Nucleic acid affinity purification was then performed, and hnRNPA2B1 amounts were measured by immunoblot. (**C**) PCR analysis of HSV-1 DNA contained in the complex immunoprecipitated by anti-hnRNPA2B1 or IgG in macrophages infected with HSV-1 (MOI, 10) for 2 hours. (**D**) Wild-type and *Hnrnpa2b1*-KO RAW264.7 cells were infected with HSV-1 (MOI, 0.5) as indicated. Viral titers in the supernatants were measured by plaque assay. (**E**) PMs from wild-type and *Hnrnpa2b1*-cKO mice were infected with HSV-1 (MOI, 1 or 10) for 6 hours for qPCR assays of *Ifnb1* mRNA (left) and 12 hours for ELISA assays of IFN-β (right) were performed. (**F** to **H**) Wild-type and *Hnrnpa2b1*-cKO mice were intraperitoneally infected with 7×10^8 PFU of HSV-1. (F) Serum IFN-β concentrations were assayed by ELISA 6 hours after HSV-1 infection. (G) Viral titers in brains 4 days after HSV-1 infection were determined by plaque assay. (H) Kaplan–Meier survival curves of mice up to 12 days after infection. Statistical significance was determined by log-rank test (n = 10 mice per group from three independent experiments). Similar results were obtained from three independent experiments. One representative experiment is shown (A) to (C). Data are displayed as means ± SEM of three [(D), (E), or (G)] or four (F) independent experiments performed in triplicate. $^{**}P < 0.01$, $^{***}P < 0.001$, two-tailed unpaired Student's t-test [(D) to (G)]. See also figs. S1 to S5.

expression were unaffected (fig. S3, A and B). Thus, hnRNPA2B1 initiates IFN-I responses to DNA viruses in both mouse and human myeloid cells.

HSV-1–induced *Ifnb1* expression decreased significantly in *Hnrnpa2b1*-knockout (KO) RAW264.7 cells (fig. S4, A and B), where HSV-1 replication was enhanced (Fig. 1D). Moreover, *Ifnb1* expression in RAW264.7 cells induced by another DNA virus adenovirus (AdV), but not by RNA viruses (SeV and VSV) or *Listeria* bacteria, was also significantly impaired by *Hnrnpa2b1* deficiency (fig. S4C). Similar results were observed in another *Hnrnpa2b1*-KO clone (fig. S4D) and in *Hnrnpa2b1*-KO L929 fibroblasts (fig. S4, E and F). Thus, hnRNPA2B1 is important for the innate immune-mediated inhibition of DNA virus replication.

Next, we established myeloid cell-specific *Hnrnpa2b1*-conditional KO (cKO) mice (fig. S4G). Upon HSV-1 infection, both the transcription and secretion of IFN-β decreased significantly in PMs deficient in *Hnrnpa2b1* (Fig. 1E). *Ifna4* transcription was also impaired, whereas the transcription of *Il6* and *Tnfa* was not (fig. S4H). Serum IFN-β concentrations were severely attenuated in *Hnrnpa2b1*-cKO mice after HSV-1 challenge (Fig. 1F). Accordingly, much higher viral titers were detected in the brains of *Hnrnpa2b1*-cKO mice after HSV-1 infection (Fig. 1G). *Hnrnpa2b1*-cKO mice also exhibited increased mortality after HSV-1 infection compared to control mice (Fig. 1H). Serum IL-6, IFN-β, and TNF-α concentrations in *Hnrnpa2b1*-cKO mice were similar to that of wild-type mice 8 hours after RNA virus SeV infection (fig. S4I). To rule out interference by other signaling pathways, we measured several major signaling molecules. cGAS, IFI16, STING, TBK1, and IRF3 amounts were comparable in both wild-type and hnRNPA2B1-KO PMs (fig. S5A). Moreover, there were similar frequencies of $F4/80^+CD11b^+$ macrophages, natural killer (NK) cells, B cells, T cells, neutrophils, and monocytes in the spleens of wild-type and *Hnrnpa2b1*-cKO mice (fig. S5B). Thus, hnRNPA2B1 plays an important role in host innate immune defense against DNA virus infection.

hnRNPA2B1 dimerization is required for its nucleocytoplasmic translocation and initiation of IFN-α/β expression

Type I interferons in antiviral innate responses are initiated by the cytoplasmic kinase TBK1 and the subsequent activation of the transcription factor IRF3 (*23*, *24*). Thus, we hypothesized that hnRNPA2B1 must be translocated to the cytoplasm to activate the TBK1–IRF3 pathway following the recognition of viral DNA in the nucleus. hnRNPA2B1 mainly localized in the nucleus but was also present in the cytoplasm 2 hours after HSV-1 infection (Fig. 2A and fig. S6A). *Hnrnpa2b1* deficiency strongly impaired the phosphorylation of TBK1 and IRF3 (Fig. 2B), as well as decreasing the kinase activity of TBK1 after HSV-1 infection (fig. S6B). Thus, we hypothesized that TBK1 was required for the hnRNPA2B1-mediated IFN-I induction. MS assays of immunoprecipitated complexes of hnRNPA2B1 or TBK1 in RAW264.7 cells infected with HSV-1 revealed an association between hnRNPA2B1 and TBK1, which was confirmed by immunoprecipitation in mouse PMs (Fig. 2C). Similar results were obtained in THP1 cells (fig. S6C), indicating that the molecular interaction was conserved in both mouse and human cells. Furthermore, hnRNPA2B1 colocalized with TBK1 in the cytoplasm after HSV-1 infection (Fig. 2D). The overexpression of hnRNPA2B1 was unable to promote HSV-1–induced IFN-β production in $Tbk1^{-/-}$ MEFs or $Irf3^{-/-}$ macrophages (fig. S6, D and E). Thus, hnRNPA2B1 acts upstream of the TBK1–IRF3 pathway to mediate IFN-β production.

Next, we investigated the mechanisms involved in driving hnRNPA2B1 nucleocytoplasmic translocation. hnRNPA2B1 dimerized after HSV-1 infection (Fig. 3A), which was confirmed by co-immunoprecipitation of Myc- and Flag-tagged hnRNPA2B1 (Fig. 3B). Mutation of the dimer interface (DI, www.ncbi.nlm.nih.gov/Structure/cdd/cddsrv.cgi; Pro^{81}, Lys^{82}, Arg^{83}, Val^{172}, Arg^{173}, Lys^{174}) in the RRM domain abrogated dimerization and nucleocytoplasmic translocation of hnRNPA2B1 in response to HSV-1 infection (Fig. 3C and fig. S7, A and B). Thus, dimerization is required for the nucleocytoplasmic translocation of hnRNPA2B1. Variants of hnRNPA2B1

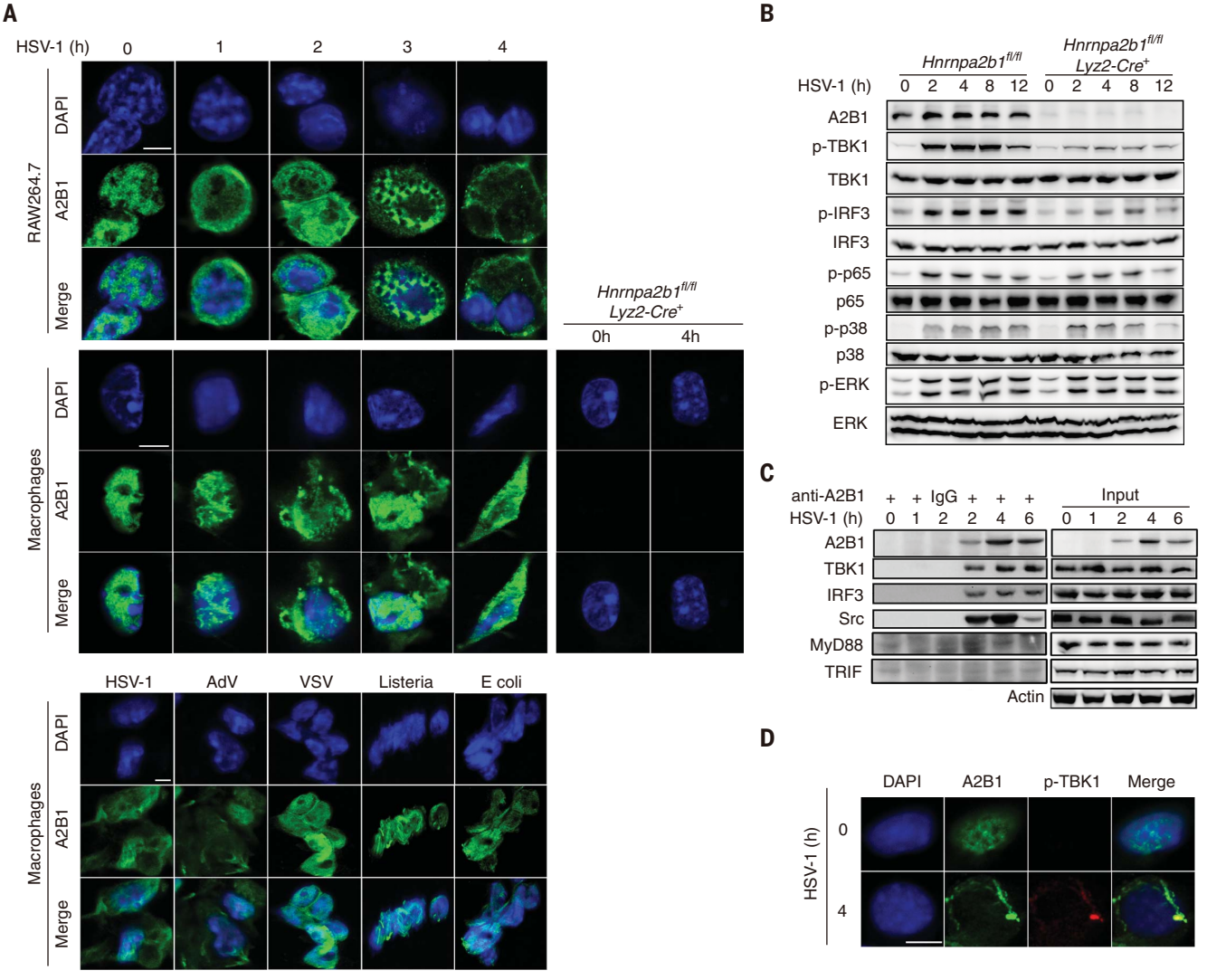

Fig. 2. DNA virus infection selectively drives nucleocytoplasmic translocation of hnRNPA2B1 to activate TBK1. (**A**) RAW264.7 cells and wild-type and *Hnrnpa2b1*-KO mouse PMs were uninfected or infected with HSV-1 (MOI, 10), AdV, VSV, *Listeria*, or *Escherichia coli* for 4 hours. hnRNPA2B1 (green) localization was then examined by confocal microscopy. Nuclei were stained with DAPI (4′,6-diamidino-2-phenylindole, blue). Scale bar, 5 μm. (**B**) PMs from wild-type and *Hnrnpa2b1*-cKO mice were infected with HSV-1 (MOI, 10) for the indicated time. Phosphorylated (p-) and total TBK1, IRF3, ERK1/2, p38, JNK, and NF-κB p65 were detected by immunoblot. (**C**) Mouse PMs were infected with HSV-1 (MOI, 10) as indicated, and cytoplasmic extracts were immunoprecipitated with anti-hnRNPA2B1 or IgG. The components in the complex were examined by immunoblot. (**D**) Confocal microscopy of colocalization of hnRNPA2B1 (green) with phosphorylated TBK1 (red) in mouse PMs infected with ultraviolet-inactivated HSV-1 (MOI, 10) for 4 hours. Nuclei were stained with DAPI (blue). Scale bar, 5 μm. Similar results were obtained for three independent experiments. One representative experiment is shown [(A) to (D)]. See also fig. S6.

carrying mutations in the dimer interface could not rescue HSV-1–induced *Ifnb1* mRNA expression (Fig. 3D) or activation of an *Ifnb1* reporter (fig. S7C). However, these dimerization mutants did not affect hnRNPA2B1 binding to viral DNA (fig. S7D). Thus, the recognition and binding of HSV-1 DNA by hnRNPA2B1 via the RRM domain appears to induce its dimerization, consequently driving its nucleocytoplasmic translocation, where it activates TBK1.

Because hnRNPA2B1 binds both viral and mammalian DNA, we examined whether hnRNPA2B1 was activated by self-DNA. Nucleofection of naked human nucleosomal DNA indeed activated *IFNB1* expression, whereas native nucleosomes did not (Fig. 3E and fig. S7E). Accordingly, hnRNPA2B1 dimers were detected after the nucleofection of naked nucleosomal DNA but not native nucleosomes (Fig. 3F). Thus, chromosomal proteins prevent the activation of hnRNPA2B1 by genomic self-DNA.

We next asked how hnRNPA2B1 activates TBK1 in response to HSV-1 infection. hnRNPA2B1 interacted with Src and STING after HSV-1 infection in mouse macrophages and human THP1 cells (fig. S8, A and B). STING and TBK1 significantly enhanced hnRNPA2B1-mediated IFN-β induction (fig. S8C). Furthermore, hnRNPA2B1 was unable to induce IFN-β in *Sting*$^{-/-}$ cells (fig. S8D). Thus, hnRNPA2B1 initiates IFN-I production by activating the STING-dependent TBK1–IRF3 pathway. Src, which has been implicated in TBK1–IRF3 activation (*25*, *26*), was activated after HSV-1 infection in mouse PMs (fig. S8E). Inhibition of Src significantly reduced serum IFN-β concentrations (fig. S8F). Thus, Src may be the upstream kinase that activates TBK1 in the hnRNPA2B1 signaling complex. As expected, phosphorylated Src colocalized with hnRNPA2B1 (fig. S8G) and active TBK1 (fig. S8H) in macrophages after HSV-1 infection. Additionally, in the absence of hnRNPA2B1, Src phosphorylation was severely impaired (fig. S8G). Src inhibitor at the concentrations used in our study did not affect HSV-1 entry into

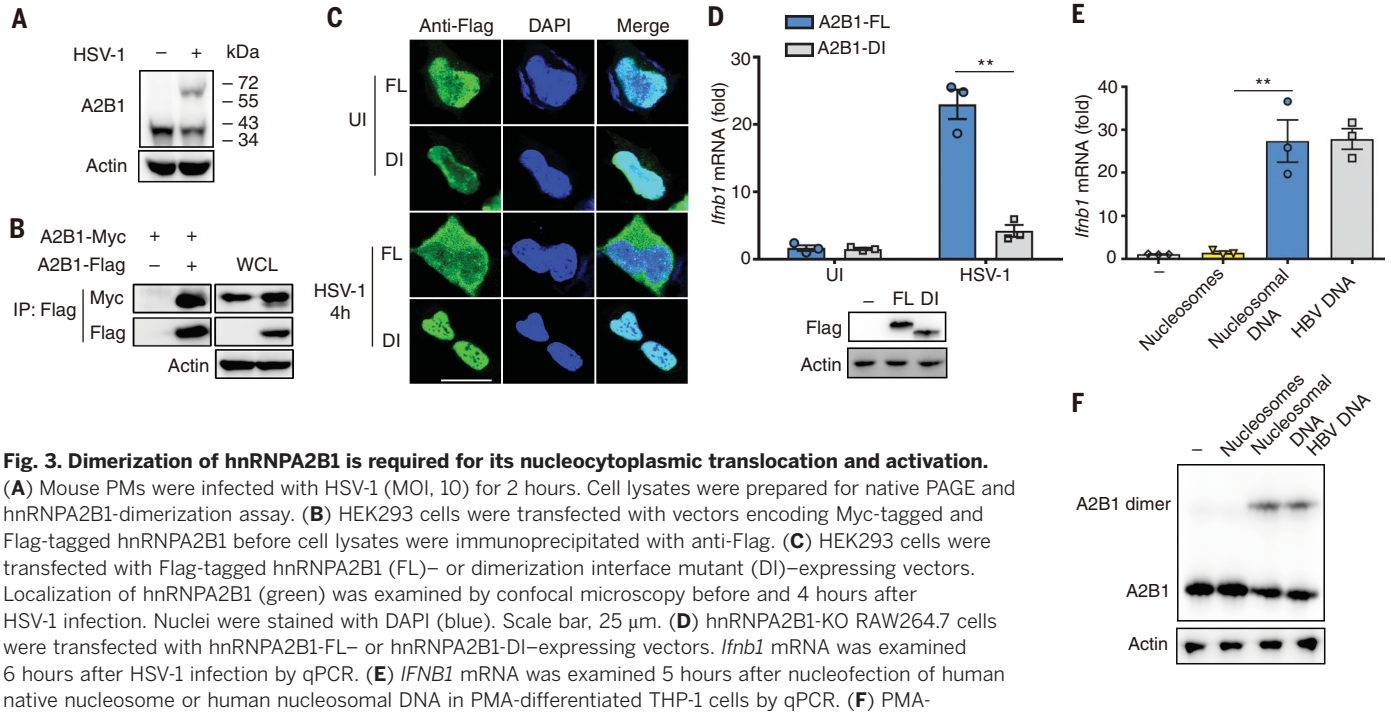

Fig. 3. Dimerization of hnRNPA2B1 is required for its nucleocytoplasmic translocation and activation. (**A**) Mouse PMs were infected with HSV-1 (MOI, 10) for 2 hours. Cell lysates were prepared for native PAGE and hnRNPA2B1-dimerization assay. (**B**) HEK293 cells were transfected with vectors encoding Myc-tagged and Flag-tagged hnRNPA2B1 before cell lysates were immunoprecipitated with anti-Flag. (**C**) HEK293 cells were transfected with Flag-tagged hnRNPA2B1 (FL)– or dimerization interface mutant (DI)–expressing vectors. Localization of hnRNPA2B1 (green) was examined by confocal microscopy before and 4 hours after HSV-1 infection. Nuclei were stained with DAPI (blue). Scale bar, 25 μm. (**D**) hnRNPA2B1-KO RAW264.7 cells were transfected with hnRNPA2B1-FL– or hnRNPA2B1-DI–expressing vectors. *Ifnb1* mRNA was examined 6 hours after HSV-1 infection by qPCR. (**E**) *IFNB1* mRNA was examined 5 hours after nucleofection of human native nucleosome or human nucleosomal DNA in PMA-differentiated THP-1 cells by qPCR. (**F**) PMA-differentiated THP-1 cells lysates were prepared for native PAGE and hnRNPA2B1 dimerization assay 2 hours after nucleofection of human native nucleosome or human nucleosomal DNA. Similar results were obtained for three independent experiments. One representative experiment is shown [(A) to (C), (F)]. Data are displayed as means ± SEM of three [(D) and (E)] independent experiments performed in triplicate. $^{**}P < 0.01$, two-tailed, unpaired Student's *t* test [(D) and (E)]. See also figs. S7 and S8.

macrophages (fig. S8I), excluding the possibility that this was due to the reduced entry of HSV-1 into macrophages. Thus, Src can bind hnRNPA2B1 and TBK1, and then activate TBK1. Together, these data demonstrate that nuclear hnRNPA2B1 forms a homodimer upon recognition of pathogen-derived DNA. This drives its translocation to the cytoplasm, where it binds and activates TBK1–IRF3 signaling via Src to initiate STING-dependent IFN-α/β expression.

JMJD6-demethylated hnRNPA2B1 dimer activates IFN-α/β expression

We next screened arginine, serine, and threonine mutations of hnRNPA2B1, and found that a mutation of Arg^{226} to Ala (R226A) within the arginine-glycine-glycine–rich (RGG) domain significantly enhanced hnRNPA2B1-induced *Ifnb1* expression (Fig. 4A). The overexpression of hnRNPA2B1-R226A in *Hnrnpa2b1*-KO RAW264.7 cells resulted in higher amounts of IFN-β mRNA and protein compared to wild-type hnRNPA2B1 (Fig. 4, B and C, and fig. S9A). Indeed, hnRNPA2B1 can be methylated at arginine residues within the RGG domain (*27*). Arginine monomethylation of hnRNPA2B1 was decreased after HSV-1 infection (Fig. 4D). Among all arginine residues, R226 was the key site for arginine monomethylation (Fig. 4E). hnRNPA2B1 was demethylated on R226 in response to HSV-1 infection in macrophages (Fig. 4F and fig. S9B). R226-demethylated hnRNPA2B1 translocated into the cytoplasm of L929 cells after HSV-1 infection (fig. S9C). Additionally, the presence of hnRNPA2B1 nuclear speckles 2 hours after HSV-1 infection suggests that hnRNPA2B1 and viral DNA colocalize. Alternatively, hnRNPA2B1 may accumulate around the nuclear pore complex when it starts to be exported into the cytoplasm. Thus, demethylation at Arg^{226} leads to hnRNPA2B1 activation and the subsequent initiation of IFN-β expression.

Our MS data suggested an association between the arginine demethylase JMJD6 and hnRNPA2B1. Immunoprecipitation experiments in mouse PMs and human THP1 cells confirmed the endogenous interaction between hnRNPA2B1 and JMJD6 upon HSV-1 infection (Fig. 5A and fig. S10A). This association was transient, as hnRNPA2B1 translocated to the cytoplasm, whereas JMJD6 remained in the nucleus (Fig. 5B). hnRNPA2B1 could be co-immunoprecipitated with JMJD6 when overexpressed in human embryonic kidney 293 (HEK293) cells (fig. S10B). JMJD6 dimerization was increased in macrophages after HSV-1 infection (fig. S10C). As the demethylation activity of JMJD6 requires its oligomerization (*28*), we hypothesized that JMJD6 may play a role in innate defense against DNA virus infection. Inhibition of JMJD6 by *N*-oxalylglycine (NOG) impaired hnRNPA2B1 demethylation in response to HSV-1 infection (Fig. 5C). HSV-1–induced *Ifnb1* expression was significantly decreased in macrophages transfected with JMJD6-specific siRNA or treated with NOG (Fig. 5D and fig. 5E). Impaired *Ifnb1* production could be rescued by the overexpression of hnRNPA2B1-R226A (Fig. 5D and fig. S10D). By contrast, JMJD6 overexpression promoted HSV-1–induced *Ifnb1* production (Fig. 5F). Thus, hnRNPA2B1 is activated by demethylation at R226 by JMJD6.

A mutation at the hnRNPA2B1 dimer interface (hnRNPA2B1-DI) led to increased arginine methylation compared to full-length hnRNPA2B1 (hnRNPA2B1-FL) (Fig. 5G). hnRNPA2B1-DI was unable to associate with JMJD6 after HSV-1 infection (Fig. 5H). Furthermore, inhibition of JMJD6 by NOG did not affect the translocation of hnRNPA2B1 in response to HSV-1 infection in macrophages (Fig. 5I). Thus, after recognizing viral DNA, hnRNPA2B1 dimerizes and then becomes demethylated by JMJD6 in the nucleus. Dimerization of hnRNPA2B1 is required for its demethylation and translocation.

hnRNPA2B1 facilitates the efficient induction of antiviral type I interferon by cGAS, IFI16, and STING

We next probed how the nuclear hnRNPA2B1 and recognized DNA sensor pathways might initiate antiviral IFN-I production. The overexpression of wild-type hnRNPA2B1 and hnRNPA2B1-R226A (the active, demethylated form of hnRNPA2B1) in $Cgas^{-/-}$ L929 cells significantly increased HSV-1–induced *Ifnb1* expression (Fig. 6A). The overexpression of hnRNPA2B1-R226A also enhanced HSV-1–induced TBK1 activation in $Cgas^{-/-}$ L929 cells (Fig. 6B), suggesting that hnRNPA2B1 can induce IFN-I at least partially in a cGAS-independent manner. This is consistent with an earlier finding that other molecules may partially compensate for the loss of cGAS (*17*).

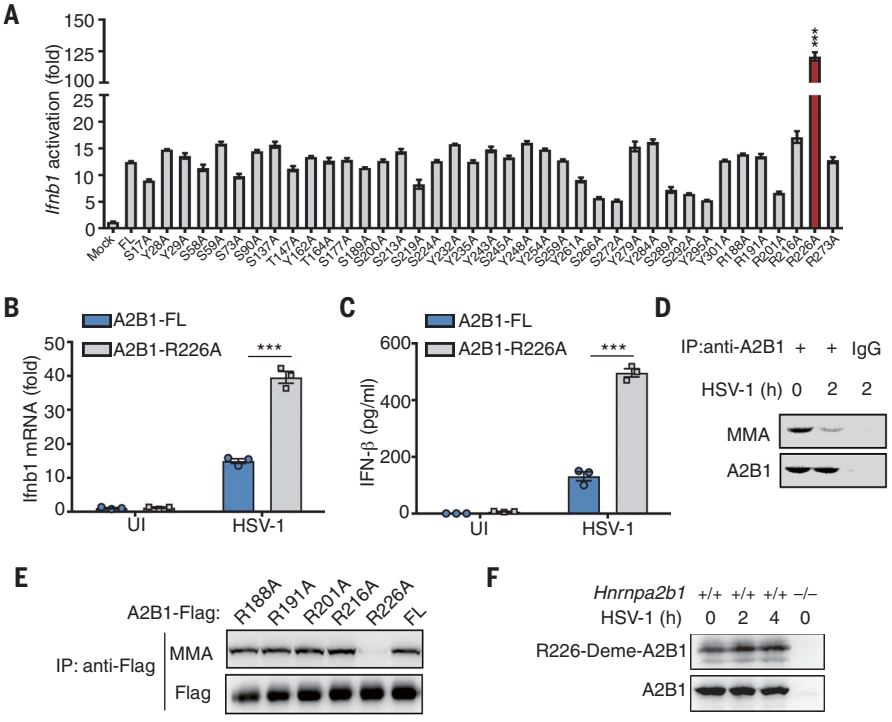

Fig. 4. Arg^{226} demethylation is essential for hnRNPA2B1-mediated type I IFN induction. (**A**) HEK293T cells were transiently transfected with hnRNPA2B1 or its mutant expression vectors with an *Ifnb1* reporter vector as indicated. The activation of the *Ifnb1* reporter was examined by dual luciferase reporter assays. (**B** and **C**) *Hnrnpa2b1*-KO RAW264.7 cells transfected with hnRNPA2B1, and mutant expression vectors were infected with HSV-1 for 7 hours (B) or 18 hours (C). *Ifnb1* mRNA was measured by qPCR (B), and IFN-β concentrations were measured by ELISA (C). (**D**) Mouse PMs were infected with HSV-1 (MOI, 10) for 2 hours. Cell lysates were immunoprecipitated with anti-hnRNPA2B1 and then examined for the level of Arg methylation by immunoblot. (**E**) HEK293T cells were transfected with the indicated vectors. Cell lysates were immunoprecipitated with anti-Flag and then examined for the level of Arg methylation by immunoblot. (**F**) The demethylation of hnRNPA2B1 was detected by using a specific antibody against R226-demethylated hnRNPA2B1 in RAW264.7 cells in response to HSV-1 infection (MOI, 10). Similar results were obtained for three independent experiments. One representative experiment is shown [(D) to (F)]. Data are displayed as means ± SEM of three [(A) to (C)] independent experiments performed in triplicate. ***P < 0.001, two-tailed, unpaired Student's t test [(A) to (C)]. See also fig. S9.

HSV-1–induced *Ifnb1* transcription was attenuated in *Hnrnpa2b1*-KO PMs (Fig. 6C). Vaccinia virus (VACV), another DNA virus, replicates in the cytoplasm and is sensed by cytosolic DNA sensors (*29*). VACV infection in *Hnrnpa2b1*-KO PMs induced *Ifnb1* production to a certain level after 4 hours but showed no subsequent increases in *Ifnb1* as it did in wild-type cells (Fig. 6C). Wild-type macrophages showed higher and more sustained *Ifnb1* expression than *Hnrnpa2b1*-KO macrophages in response to both viruses (Fig. 6C). Similar results were obtained in BMDMs (fig. S11). Thus, hnRNPA2B1 appears to be required for cGAS-, IFI16-, and STING-mediated pathways to fully activate type I interferon production against DNA viruses.

hnRNPA2B1 promotes nucleocytoplasmic trafficking of CGAS, IFI16, and STING mRNAs to amplify cytoplasmic innate sensor signaling

We next investigated why hnRNPA2B1 is required for the efficient induction of IFN-I by cGAS, IFI16, and STING in response to HSV-1 infection. Up to 6 hours after HSV-1 infection, the endogenous amounts of cGAS, p204 (the functional mouse ortholog of human IFI16), and STING protein were similar in both wild-type and *Hnrnpa2b1*-KO RAW264.7 cells. cGAS expression began to increase in wild-type RAW264.7 cells 6 hours after infection, whereas p204 began to increase 12 hours after infection. However, these proteins failed to increase in *Hnrnpa2b1*-KO RAW264.7 cells following HSV-1 infection (Fig. 6D). STING abundance decreased more rapidly in *Hnrnpa2b1*-KO RAW264.7 cells than in wild-type RAW264.7 cells 6 hours after infection (Fig. 6D). Thus, hnRNPA2B1 appears to be required for the efficient induction of cGAS, IFI16, and STING after DNA virus infection, which subsequently generates an antiviral IFN-I response.

We examined the effects of hnRNPA2B1 on *Cgas*, *p204*, and *Sting* mRNA expression. The transcriptional levels of these genes were similar in wild-type and *Hnrnpa2b1*-KO RAW264.7 cells, indicating that the splicing of these mRNAs was unaffected (fig. S12A). Similarly, the stability of these mRNAs did not significantly differ between these cell lines (fig. S12B). However, depletion of hnRNPA2B1 led to the nuclear retention of *Cgas*, *p204*, and *Sting* mRNAs (Fig. 7A). Analysis of mRNAs associated with hnRNPA2B1-immunoprecipitated complexes revealed that hnRNPA2B1 was able to bind *Cgas*, *p204*, and *Sting* mRNAs in macrophages after HSV-1 infection (Fig. 7B). Thus, hnRNPA2B1 appears to play a role in mediating the nucleocytoplasmic translocation of these mRNAs.

N6-methyladenosine (m^{6}A) is the predominant methylated base in mammalian mRNAs and has been recently revealed to promote mRNA translocation from the nucleus to the cytoplasm (*30*, *31*). A greater number of methylated mRNAs were precipitated after HSV-1 infection, although the amounts of methylated *Cgas*, *p204*, and *Sting* mRNA were much lower in *Hnrnpa2b1*-KO RAW264.7 cells than in controls (Fig. 7C). Thus, specific classes of mRNAs involved in antiviral response such as *Cgas, p204*, and *Sting*, undergo m^{6}A modification after DNA virus infection in an hnRNPA2B1-dependent manner.

Two RNA demethylases, alkylated DNA repair protein alkB homolog 5 (ALKBH5) and fat mass and obesity-associated protein (FTO), have been identified to date (*31*, *32*). Our MS data suggested an interaction between hnRNPA2B1 and FTO. hnRNPA2B1 was constitutively associated with FTO, and hnRNPA2B1 disassociated with FTO after HSV-1 infection in mouse PMs and human THP1 cells (Fig. 7D and fig. S12C). Knockdown of FTO led to increased HSV-1–induced *Ifnb1* expression in macrophages (Fig. 7E and fig. S12D).

The METTL3–METTL14 complex mediates mRNA m^{6}A methylation. To explore whether METTL3 was involved in the innate immune response, we studied myeloid cell–specific *Mettl3*-KO mice (*33*). *Ifnb1* expression was impaired in *Mettl3*-KO PMs and BMDMS after HSV-1 infection (fig. S12E). METTL3 deficiency did not affect hnRNPA2B1 binding with *Cgas*, *p204*, or *Sting* mRNAs (fig. S12F). *Cgas*, *p204*, and *Sting* m^{6}A levels were lower in *Mettl3*-KO macrophages than in wild-type cells (fig. S12G). Thus, METTL3 contributes to the m^{6}A modification of hnRNPA2B1-bound mRNAs in macrophages, which promotes IFN-β expression in response to DNA virus infection.

The binding of *CGAS, IFI16*, and *STING* mRNAs by demethylated hnRNPA2B1 was severely impaired compared to that by hnRNPA2B1-FL (Fig. 7F and fig. S12H). The m^{6}A levels of these mRNAs in JMJD6 inhibitor-treated cells were similar to control cells (Fig. 7G). Thus, RNA binding by hnRNPA2B1 requires Arg^{226} methylation, and demethylated hnRNPA2B1 cannot bind these mRNAs or affect their m^{6}A modification.

Analysis of RNA from nuclear and cytoplasmic fractions in both wild-type and *Hnrnpa2b1*-KO macrophages before and after HSV-1 infection revealed that hnRNPA2B1 deficiency decreased the nuclear export of mRNAs involved in several biological processes, including pheromone

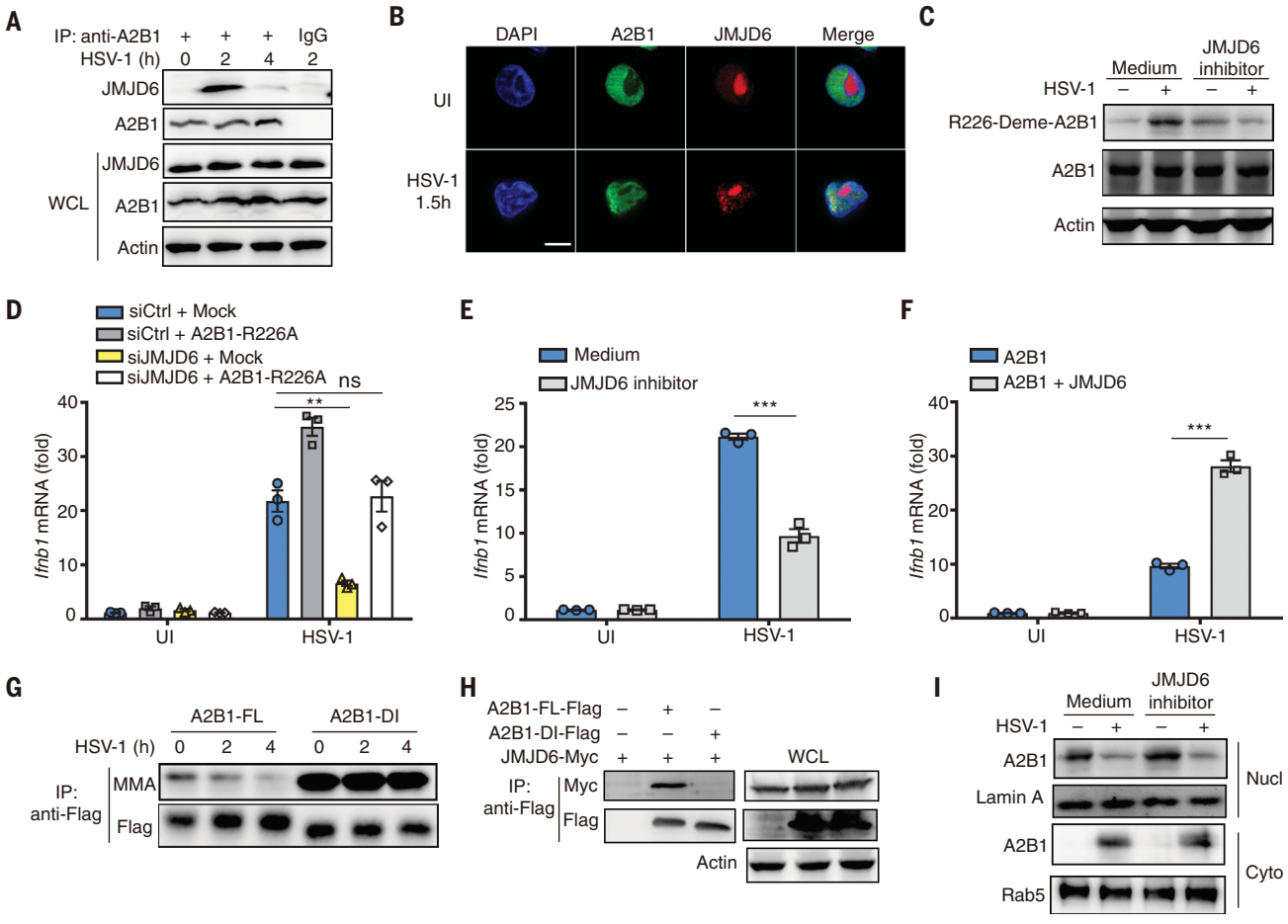

Fig. 5. JMJD6-mediated demethylation is essential for hnRNPA2B1-mediated type I IFN induction. (**A**) Mouse PMs were infected with HSV-1 (MOI, 10). Cell lysates were immunoprecipitated with anti-hnRNPA2B1 or IgG. The components in the complex were examined by immunoblot. (**B**) Mouse PMs infected with HSV-1 (MOI, 10) for 1.5 hours were examined for hnRNPA2B1 (green) and JMJD6 (red) by confocal microscopy. Nuclei were stained with DAPI (blue). Scale bar, 5 μm. (**C**) The demethylation of hnRNPA2B1 was detected by using a specific antibody against R226-demethylated hnRNPA2B1 in RAW264.7 cells after HSV-1 infection (MOI, 10) with or without JMJD6 inhibitor treatment. (**D**) Mouse PMs transfected with control siRNA or JMJD6-specific siRNAs were transfected with mock or hnRNPA2B1-R226A-expressing vector and infected with HSV-1 (MOI, 10) for 7 hours. *Ifnb1* mRNA was examined by qPCR. (**E**) Mouse PMs treated with or without JMJD6 inhibitor for 2 hours were infected with HSV-1 (MOI, 10). The *Ifnb1* mRNA was examined by qPCR. (**F**) RAW264.7 cells transfected with plasmids encoding hnRNPA2B1 or JMJD6 were infected with HSV-1 (MOI, 10). The *Ifnb1* mRNA was examined by qPCR. (**G**) HEK293T cells were transfected with Flag-tagged hnRNPA2B1-FL or -DI. Cell lysates were immunoprecipitated with anti-Flag and examined for Arg methylation by immunoblot. MMA, monomethylated arginines. (**H**) HEK293T cells were transfected with Flag-tagged hnRNPA2B1-FL or -DI and Myc-tagged JMJD6. Cell lysates were immunoprecipitated with anti-Flag and examined for Myc by immunoblot. (**I**) RAW264.7 cells were treated with or without JMJD6 inhibitor for 2 hours and then were infected with HSV-1 (MOI, 10) as indicated, and the cytoplasmic and nuclear proteins were separated. The subcellular distribution of hnRNPA2B1 was examined by immunoblot. Similar results were obtained in three independent experiments, and one representative was shown [(A) to (C), (G) to (I)]. Data are displayed as means ± SEM of three [(D) to (F)] independent experiments performed in triplicate. $^{**}P < 0.01$, $^{***}P < 0.001$; ns, not significant; two-tailed, unpaired Student's *t* test [(D) to (F)]. See also fig. S10.

receptor activity and electron transfer activity (fig. S13A). Several immune-associated genes including *Cgas* and *Sting* mRNAs were retained within the nucleus in macrophages after HSV-1 infection. By contrast, most housekeeping genes, such as *Actb* and *Gapdh*, were unaffected. Thus, not all genes were regulated by hnRNPA2B1 (fig. S13B). hnRNPA2B1 regulated more innate immune-associated genes than adaptive immune-associated genes (fig. S13C). hnRNPA2B1 appeared to affect a set of genes involved in several innate processes, including antigen presentation, the complement system, cytokine and chemokine signaling, and interferon responses (fig. S13D). Thus, hnRNPA2B1 plays a role in regulating the export of immune-associated RNAs after HSV-1 infection, especially genes involved in innate immune activation.

In conclusion, these findings suggest a dynamic interaction between hnRNPA2B1 and FTO. This interaction, in turn, affects the m^6A modification of *CGAS*, *IFI16*, and *STING* mRNAs and modulates their nucleocytoplasmic trafficking and translation in response to DNA virus infection. Thus, hnRNPA2B1 plays a crucial role in shaping the antiviral innate immune response.

Discussion

The mechanisms by which viral nucleic acids are surveilled are largely unknown. Here, we identify and validate hnRNPA2B1 as a nuclear viral DNA sensor through a series of in vitro and in vivo experiments using myeloid cell–specific *Hnrnpa2b1*-KO mice established for this study. The activities of hnRNPA2B1 illustrate the complexity, diversity, and flexibility of the nuclear innate immune response, which is at least as elaborate as cytoplasmic immune signaling. More intensive future efforts are warranted to fully understand the functional importance of nuclear

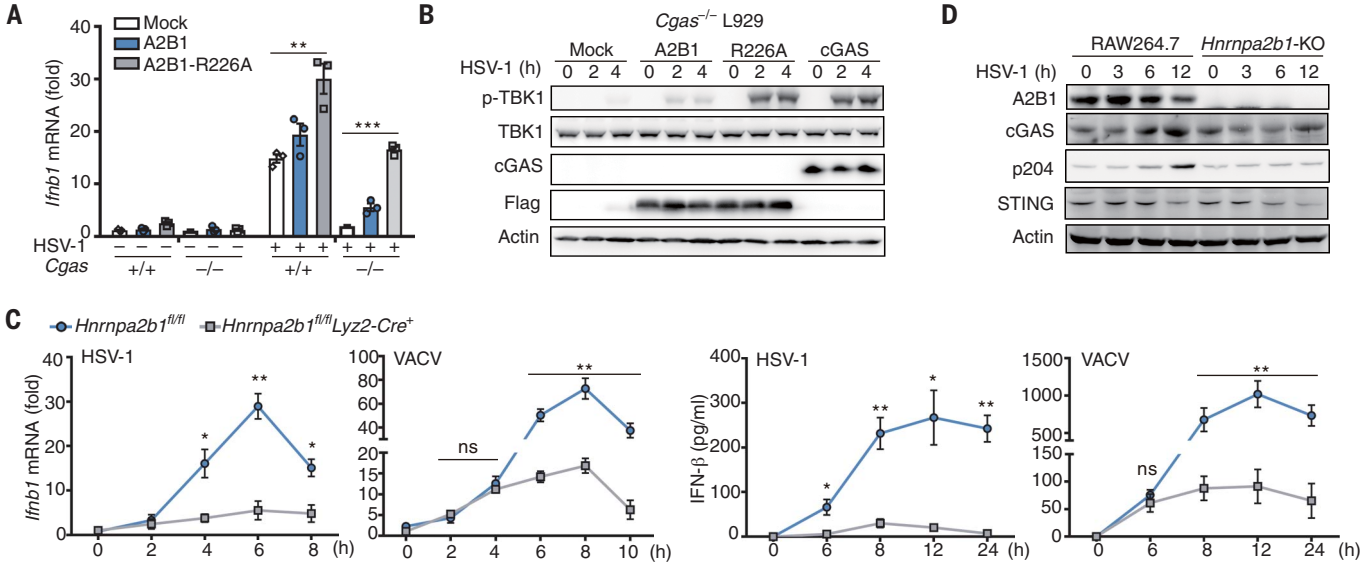

Fig. 6. hnRNPA2B1 is required for efficient type I interferon induction by cGAS, IFI16, and STING. (**A**) Wild-type and *Cgas*$^{-/-}$ L929 cells were transfected with mock, hnRNPA2B1, or hnRNPA2B1-R226A vectors for 24 hours, respectively, and then infected with HSV-1 (MOI, 10) for 7 hours. *Ifnb1* mRNA was assayed by qPCR. (**B**) Wild-type and *Cgas*$^{-/-}$ L929 cells were transfected with mock, Flag-hnRNPA2B1, Flag-hnRNPA2B1-R226A, or cGAS vectors, respectively, for 24 hours and then infected with HSV-1 (MOI, 10) as indicated. TBK1 activation was assayed by immunoblot. (**C**) Wild-type and *Hnrnpa2b1*-KO PMs were infected with HSV-1 (MOI, 1) or VACV (MOI, 1) as indicated. *Ifnb1* mRNA was assayed by qPCR and the amount of IFN-β protein was assayed by ELISA. (**D**) Wild-type and *Hnrnpa2b1*-KO RAW264.7 were infected with HSV-1 (MOI, 10) as indicated. Whole-cell lysates were prepared and examined by immunoblot for cGAS, STING, and p204 expression. Similar results were obtained for three independent experiments. One representative experiment is shown [(B) and (D)]. Data are displayed as means ± SEM of three [(A) and (C)] independent experiments performed in triplicate. *P < 0.05, **P < 0.01, ***P < 0.001; ns, not significant; two-tailed, unpaired Student's t test [(A) and (C)]. See also fig. S11.

response pathways in innate immunity and inflammation.

cGAS has been shown to have an essential role for innate response to pathogenic DNA. cGAS recognizes viral DNA in the cytoplasm, whereas hnRNPA2B1 senses viral DNA in the nucleus and initiates IFN signaling at least partially independent of cGAS. These two sensors cooperatively anchor an integrated cellular pathogen-sensing system with other known cytoplasmic sensors. We found that the overexpression of hnRNPA2B1 can increase HSV-I–induced TBK1 activation and IFN-β production in cGAS KO cells, but not increase HSV-1–induced IFN-β production in *Sting*$^{-/-}$, *Tbk1*$^{-/-}$, or *Irf3*$^{-/-}$ cells. In response to DNA virus infection, hnRNPA2B1 initiates the STING-dependent activation of TBK1-IRF3 for IFN-I production, but not NF-κB activation for IL-6 and TNF-α production. Additionally hnRNPA2B1 promotes the translocation of immune-associated mRNAs, including *CGAS*, *IFI16*, and *STING* mRNAs, and subsequently enhances their expression, ensuring the robust integration of innate immune responses. Thus, hnRNPA2B1 activity represents an important host defense mechanism by which innate antiviral responses are initiated and amplified. Our findings add insight into how this network of cellular DNA sensors efficiently launch and license innate immune responses to DNA viruses.

We found that the dimerization and dimerization-dependent demethylation mode determines whether hnRNPA2B1 functions as an IFN initiator or amplifier. In response to DNA virus infection, hnRNPA2B1 dimerizes and undergoes Arg^{226} demethylation. Demethylated hnRNPA2B1 translocates to the cytoplasm to initiate IFN-α/β production. The nuclear transport and activation of many signaling molecules requires dimerization, such as in the cases of signal transducer and activator of transcription 1 (STAT1) and STING. Here, we demonstrate that only dimerized hnRNPA2B1 can translocate to the cytoplasm. This dimer-only export of signaling molecules may be a key checkpoint for immune surveillance.

Accumulating evidence shows that there is precise epigenetic control of innate immunity (*34*). For instance, we previously demonstrated that the RNA helicase DDX46 recruits ALKBH5 to demethylate the m^{6}A of *Mavs*, *Traf3*, and *Traf6* transcripts after viral infection, consequently enforcing their retention in the nucleus and preventing their translation, which, in turn, inhibits the antiviral interferon response (*35*). hnRNPA2B1 has been primarily studied as an RNA-binding protein (RBP) (*36*–*38*). We report here that hnRNPA2B1 can also function as an m^{6}A "modulator" to promote the m^{6}A modification and nucleocytoplasmic trafficking of *CGAS*, *IFI16*, and *STING* mRNAs in response to DNA virus infection, leading to the enhanced production of type I interferons. These findings demonstrate an important role for mRNA m^{6}A modification in innate immune responses. Additional RBPs may also engage in DNA binding and affect associated biological processes.

hnRNPA2B1 binds both viral and mammalian DNA. Self genomic DNA is normally wrapped and protected by chromosomal protein complexes to prevent self-recognition. Similar mechanisms may potentially be exploited by DNA viruses by forming minichromosomes to escape sensing. cGAS and IFI16 play a role in systemic lupus erythematosus (SLE) (*39*–*42*). Similarly, autoantibodies against hnRNP-A2 have been observed in patients with SLE (*43*). A more detailed understanding of the interactions between hnRNPA2B1, pathogen-derived DNA, and host genomic DNA in physiological and pathological conditions will be necessary.

Thus, we hypothesize a highly ordered biological circuit, which critically involves hnRNPA2B1. The protein maintains its regular functions in association with RNA in the resting, infection-free state. However, upon recognizing "foreign" DNA in the nucleus, hnRNPA2B1 polarizes its function to be a nuclear sensor for viral DNA and activates innate immune response by two integrated biological functions: initiating the IFN-I response by activating TBK1 in the cytoplasm and amplifying innate signaling by regulating the transport of innate immune mRNAs in parallel or sequence. The functional "polarization" of hnRNPA2B1 then allows cells to initiate an innate immune defense program to counter DNA viruses. The nature and purpose of hnRNPA2B1 dimerization after foreign DNA

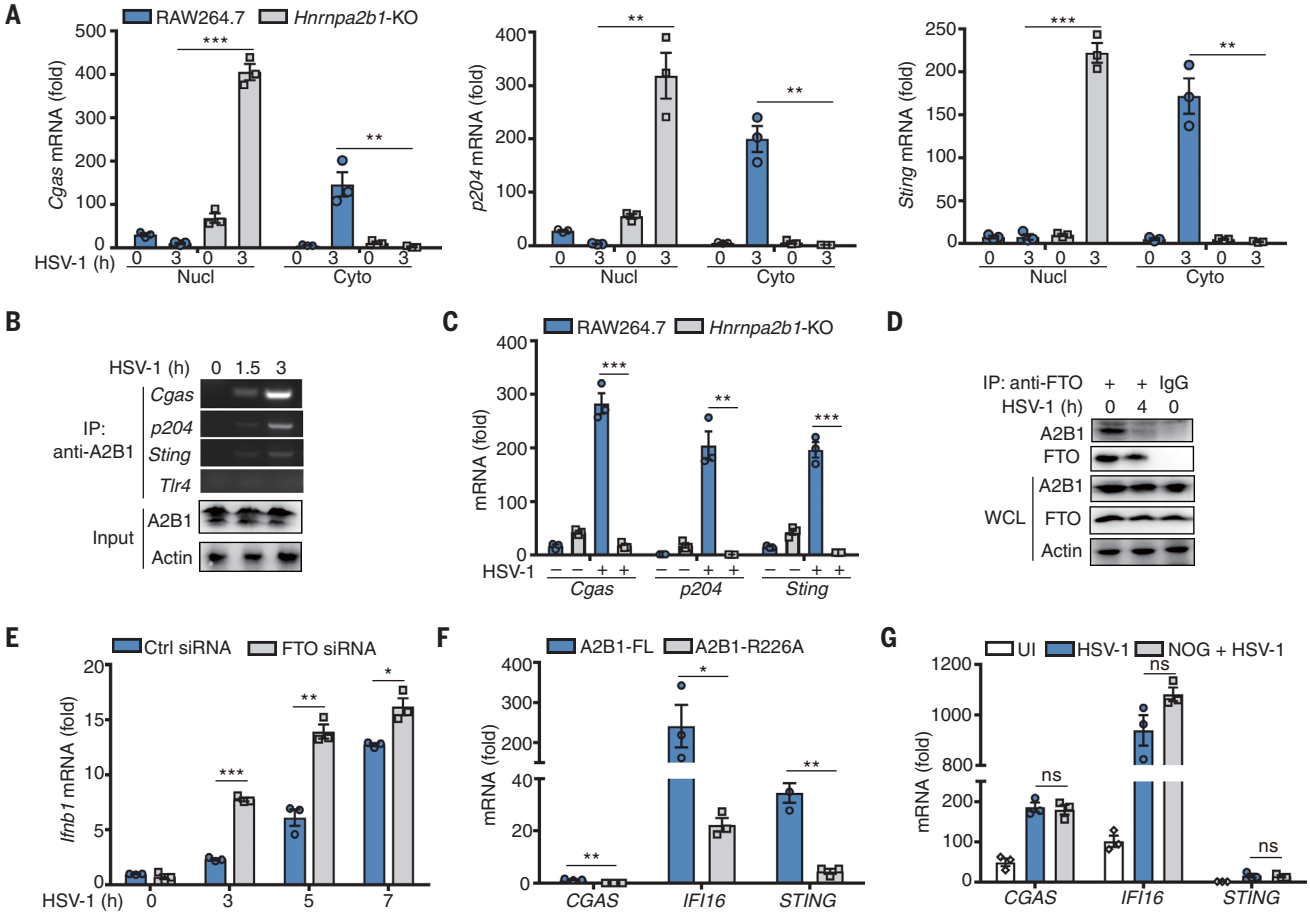

Fig. 7. hnRNPA2B1 facilitates m^{6}A modification and nucleo-cytoplasmic trafficking of *CGAS*, *IFI16*, and *STING* mRNAs upon DNA virus infection. (**A**) Wild-type and *Hnrnpa2b1*-KO RAW264.7 cells were infected with HSV-1 (MOI, 10) as indicated, and the cytoplasmic or nuclear mRNAs were extracted. *Cgas*, *p204*, and *Sting* mRNAs were detected by qPCR. The distribution of mRNA was analyzed quantitatively by densitometry of indicated mRNAs in the nucleus and cytoplasm relative to *Actb*. (**B**) Mouse PMs were infected with HSV-1 (MOI, 10) as indicated. hnRNPA2B1 was immunoprecipitated and mRNAs in the complex were detected using specific primers by PCR. (**C**) m^{6}A-containing mRNAs were immunoprecipitated with anti-m^{6}A from equal amounts of total mRNAs from wild-type and hnRNPA2B1-KO RAW264.7 cells with or without HSV-1 infection (MOI, 10) for 3 hours. *Cgas*, *p204*, and *Sting* mRNAs were assayed by qPCR. (**D**) Mouse PMs were infected with HSV-1 (MOI, 10) as indicated, and cellular extracts were immunoprecipitated with anti-FTO. hnRNPA2B1 was examined by immunoblot. (**E**) Mouse PMs transfected with control siRNA or FTO-specific siRNA were infected with HSV-1 (MOI, 10) as indicated. *Ifnb1* mRNA expression was examined by qPCR. (**F**) mRNAs were immunoprecipitated with anti-Flag from equal amounts of total mRNAs from overexpressed hnRNPA2B1-FL and -R226A HEK293 cells with or without HSV-1 infection (MOI, 10) for 3 hours. *CGAS*, *IFI16*, and *STING* mRNAs were assayed by qPCR. (**G**) m^{6}A-containing mRNAs were immunoprecipitated with anti-m^{6}A from equal amounts of total mRNAs from PMA-differentiated THP-1 cells with or without NOG treatment. Cells were infected with HSV-1 infection (MOI, 10) for 3 hours. *CGAS*, *IFI16*, and *STING* mRNAs were assayed by qPCR with specific primers. Similar results were obtained for three independent experiments. One representative experiment is shown [(B) and (D)]. Data are displayed as means ± SEM of three [(A), (C), (E) to (G)] independent experiments performed in triplicate. *P < 0.05, **P < 0.01, ***P < 0.001; ns, not significant; two-tailed, unpaired Student's t test [(A), (C), (E) to (G)]. See also figs. S12 and S13.

recognition remain open questions. Furthermore, the differences between the DNA- and RNA-binding activities of hnRNPA2B1 are still unknown. In conclusion, this study strongly suggests that nuclear DNA sensors such as hnRNPA2B1 are essential contributors to innate immune defense.

Materials and methods

Mice

C57BL/6 mice were purchased from Joint Ventures Sipper BK Experimental Animal (Shanghai, China). *Lyz2*-Cre mice were purchased from The Jackson Laboratory. To establish *Hnrnpa2b1*-conditional-knockout mice, exons 2 to 6 of the *Hnrnpa2b1* gene were trapped by insertion of loxP sequences which can be specifically recognized by CRE recombinase. *Hnrnpa2b1*$^{fl/fl}$ mice were backcrossed onto C57BL/6J background, and then crossed with *Lyz2*-Cre mice. Exons 2 to 6 were excised by CRE recombinase in myeloid cells. *Hnrnpa2b1*$^{fl/fl}$*Lyz2-Cre*$^{+/-}$ mice were mated with *Hnrnpa2b1*$^{fl/fl}$*Lyz2-Cre*$^{-/-}$ mice to generate *Hnrnpa2b1*$^{fl/fl}$*Lyz2-Cre*$^{+}$ and littermate control mice for further experiments. The mice were bred in specific pathogen-free conditions. Mice bearing a *Mettl3*^{fl} allele (*Mettl3*^{fl} mice) were from Q. Zhou (Chinese Academy of Sciences, China) and were crossed with *Lyz2*-Cre mice to obtain *Mettl3*$^{fl/fl}$*Lyz2-Cre*$^{+}$ mice. Mice at 8 weeks of age were used for in vivo experiments.

All animal experiments were undertaken in accordance with the National Institute of Health Guide for the Care and Use of Laboratory Animals, with the approval of the Second Military Medical University, Shanghai.

Cells and reagents

RAW264.7 cells, HEK293 cells, and HEK293T cells were obtained from ATCC and cultured in Dulbecco's modified Eagle's medium (DMEM) medium with 10% (v/v) fetal bovine serum (FBS)

(Gibco). Mouse peritoneal macrophages were isolated from the peritoneal cavities of mice 3 days after injection with thioglycolate medium and cultured in (DMEM) medium with 10% (v/v) FBS. *Cgas*$^{-/-}$ L929 cells and plasmids encoding *CGAS*, *STING* and *IFI16* were from Z. J. Chen (University of Texas Southwestern Medical Center). *Sting*$^{-/-}$ BMDMs and *Tbk1*$^{-/-}$ MEFs were from G. Cheng (UCLA).

VSV was a gift from W. Pan (Second Military Medical University, Shanghai, China), and Sendai virus was from B. Sun (Chinese Academy of Sciences, Shanghai, China).

Antibodies specific to hemagglutinin (HA)–tag (ab1424), Flag-tag (ab18230), Actin (Abcam 8226), cGAS (ab176177), IFI16 (ab104409) JMJD6 (ab64575) and STING (ab92605), the recombinant IRF3 (ab132091), were from Abcam Inc (Cambridge, MA). ANTI-FLAG M2 Magnetic Beads (M8823) and *N*-oxalylglycine (NOG) were from Sigma-Aldich (St. Louis, MO). Src inhibitor Saracatinib was from Selleck (Houston, TX). Antibodies specific for monomethyl arginine (Me-R4-100) (8015), IRF3 (4302), p65 (8242), Src (2123) and TBK1 (3504), and phospho-specific antibodies against IRF3 (Ser396) (4947), Src (Tyr416) (6943), TBK1 (Ser172) (5483) were from Cell Signaling Technology (Beverly, MA). Antibody against hnRNPA2B1 (anti-hnRNPA2B1) (sc-374053) was from Santa Cruz Biotechnology (Dallas, TX). Antibody specific for demethylated hnRNPA2B1 (R226) was developed using synthesized antigenic 14–amino acid peptide of deme-hnRNPA2B1 (R226): CDGYGSGRGFGDGY. Rabbit polyclonal antibodies to the peptide were purified using protein A. Finally, antibody specificity was validated using dot blot analysis.

For immunoblotting, anti-cGAS was used at 1.2 μg/ml, anti-JMJD6 at 1 μg/ml, and anti-STING at 0.5 μg/ml, and other antibodies were used at a concentration of 0.2 μg/ml. For immunofluorescence, antibodies were used at a concentration of 2 μg/ml.

HSV-1 DNA purification, biotin labeling and nucleic acid affinity purification

HSV-1 genomic DNA was purified by using ChargeSwitchg DNA Preparation Kit (Invitrogen, San Diego, CA). Approximately 5 pmol of purified viral DNA was biotinylated with a biotin 3′-end DNA labeling kit (89818, Pierce Biotechnology, Rockford, IL). Nuclear extracts from RAW264.7 cells were prepared using the Nuclear Complex Co-IP Kit (54001, Active Motif, Carlsbad, CA). Nuclear extracts were incubated with biotinylated HSV-1 DNA at 4°C overnight. The complexes were precipitated on streptavidin-coupled dynabeads (Invitrogen, 601.01), washed four times with phosphate-buffered saline (PBS) buffer and resolved on 10% SDS–PAGE gel. Differential protein bands were then selected for MS assays after silver staining.

2D electrophoresis

Nuclear and cytoplasmic extracts from RAW264.7 cells with or without infection of HSV-1 or VSV were separated on 2D SDS–PAGE gels. Isoelectric focusing was performed with ZOOM IPGRunner Kit (Invitrogen). Zoom Stripes with a pH 3 to 10 range were used overnight followed by SDS–PAGE. After silver staining, each gel was scanned on a Typhoon 9410 scanner (GE Healthcare). Each differential gel spot was excised for protein identification.

Nanospray liquid chromatography–tandem mass spectrometry

Proteins in selected bands (dots) derived from nucleic acid affinity purification, 2D electrophoresis, or immunoprecipitations were eluted and digested. Digests were analyzed by nano-ultra-performance liquid chromatography–electrospray ionization tandem mass spectrometry. Data from liquid chromatography–tandem mass spectrometry were processed through the use of ProteinLynx Global Server version 2.4 (PLGS 2.4); the resulting peak lists were used for searching the NCBI protein database with the Mascot search engine.

Sequences, plasmids constructs, transfection and RNA interference

The recombinant vectors encoding *Hnrnpa2b1* (GenBank No. NM_182650) and its mutants were constructed by PCR-based amplification from RAW264.7 cDNA and then subcloned into the pcDNA3.1 eukaryotic expression vector (Invitrogen). The pRL-TK-Renilla-luciferase plasmid was obtained from Promega (Madison, WI). Mouse DNAs for *Ifnb1* promoter were amplified from RAW264.7 cells by PCR and cloned into pGL3 plasmid (Promega) to construct *Ifnb1* luciferase reporter plasmids. The primers were: 5′-AGCTTGAATAAAATGCTAGCTAGAAGCTGTTAGAA-3′ and 5′-CAAGATGAGGCAAAGCTTCAAAGGCTGCAGTGAGAAT-3′. All constructs were confirmed by DNA sequencing.

For transient transfection of plasmids, the jetPEI reagents were used (Polyplus-transfection Company, Illkirch, France). For transient silence, the siRNA duplexes were transfected using INTERFERin reagent (Polyplus-transfection Company) according to the standard protocol. The target sequences used for transient silence were as follows: 5′-GAGGAAATTATGGAAGTGG-3′ and 5′-CCACAGAAGAAAGTTTGAGTT-3′ (siRNA2) for mouse hnRNPA2B1; 5′-CTTTGGTGGTAGCAGGAAC-3′ for human hnRNPA2B1; and 5′ CTGTGAAAGTGTATGAGAA-3′ for TBK1; 5′-TGAAGCAATTACCTGGTTTAA-3′ and 5′-GTTATCAAGGAAGTGGTATAG-3′ for mouse JMJD6; 5′-CAACGTGACTTTGCTAAAC-3′ for mouse FTO. The nonsense sequence 5′-TTCTCCGAACGTGTCACGT-3′ was used as a control siRNA.

Assay of luciferase reporter gene expression

Cells were cotransfected with the mixture of *Ifnb1* luciferase reporter plasmid, RL-TK-Renilla-luciferase plasmid, and the indicated constructs. Luciferase activities were measured with Dual-Luciferase Reporter Assay System (Promega) according to the manufacturer's instructions. Data were normalized for transfection efficiency by dividing Firefly luciferase activity with that of Renilla luciferase.

Determination of HSV-1 replication

To assess the replication of HSV-1, we infected the indicated RAW264.7 cells and L929 cells with HSV-1 [multiplicity of infection (MOI), 0.5] and the viral titers were measured by plaque assays.

In vitro kinase assay

Whole cell lysates (100 μg) were incubated with 2 ng of anti-TBK1 or immunoglobulin G (IgG) with gentle rocking at 4°C overnight. Protein G magnetic beads (Millipore) were added and incubated for additional 4 hours. The kinase activity of TBK1 was measured by using Universal Kinase Activity Kit (EA004, R&D Systems) in the presence of recombinant IRF3 as instructed.

Nucleofection

Phorbol 12-myristate 13-acetate (PMA)–differentiated THP-1 cells were transfected with 1 μg of human native nucleosomes (Millipore, 14-1057), DNA extracted from human native nucleosomes, or HBV DNA, by Amaxa Nucleofector following the manufacturer's instructions. To confirm that DNA bound to the native nucleosomes reaches the nucleus, we transfected THP1 cells with 1 μg of chicken native nucleosomes (Epicypher, 16-0019). Nuclear fractions were then separated and DNA was extracted for qPCR with chicken-specific primers.

Affymetrix GeneChip analysis

Wild-type and *Hnrnpa2b1* knockout peritoneal macrophages were infected with HSV-1 (MOI, 10) for 4 hours. RNAs from the nuclear fraction and the cytoplasmic fraction from both kinds of cells was isolated using TRIZOL. RNA samples were deoxyribonuclease I (DNase I)–treated, labeled, and hybridized on mouse GeneChip 1.0 ST arrays (Affymetrix) following standard procedures. After scanning (GeneChip Scanner 3000 7G; Affymetrix) of the arrays, the CEL files generated were analyzed using BRB Array Tool and processed using the RMA algorithm (robust multi-array average) for normalization and summarization. Gene expression ratios were processed and visualized as a heatmap.

Immunoprecipitation

For immunoprecipitation, 1 μg of specific antibodies or IgG was added per 1 mg of total proteins (1 ml of whole cell lysates) and then incubated with gentle rocking at 4°C overnight. The complexes were precipitated with Protein G magnetic beads (MILLIPORE, LSKMAGG02).

Measurements of cytokine production

Cytokine mRNA levels were assayed by quantitative real-time PCR via LightCycler (Roche, Basel, Switzerland) and SYBR RT-PCR kit (Takara, Dalian, China).

Cytokine protein levels were measured with ELISA Kits (R&D Systems, Minneapolis, MN) according to the manufacturer's instructions.

HSV-1 entry detection

Mouse peritoneal macrophages were treated with or without Src inhibitor for 30 min and infected with HSV-1 (MOI, 10) as indicated. One hour later, supernatants were removed and cells were washed with PBS for two times. Whole cell lysates were then subjected to SDS–PAGE and immunoblotted using an anti-HSV-1 major capsid protein VP5 antibody (Santa Cruz, sc-13525).

Confocal microscopy

RAW264.7 cells, HEK293 cells or L929 cells, plated on glass coverslips in six-well plates, were left uninfected or infected with HSV-1 or indicated pathogens. After being fixed in 4% (wt/vol) paraformaldehyde and treated with 0.5% (vol/vol) Triton X-100, cells were stained with primary antibodies (2 μg/ml) overnight at 4°C and then with Alexa Fluor 488- and 568-labeled secondary antibodies for 2 hours at room temperature. Cells were stained with or 4',6-diamidino-2-phenylindole (DAPI) for 5 min at room temperature and then observed with a Leica TCS SP8 confocal laser microscope with 63×/1.40 oil objective lens. Images were processed using Leica Application Suite X software (LAS X, V2.0.2.15022).

In vivo modulation of HSV-1 infection

Hnrnpa2b1$^{fl/fl}$ and *Hnrnpa2b1*$^{fl/fl}$*Lyz2-Cre*$^{+}$ mice were infected with 1×10^{8} plaque-forming units (PFU) of HSV-1 viruses intraperitoneally. Serum IFN-β concentrations were determined by enzyme-linked immunosorbent assay (ELISA) kit. HSV-1 titers were determined by plaque assays using homogenates from brains of infected mice.

Densitometry analysis

Gels were scanned by Tanon 3500B Gel Image System (Tanon, Shanghai, China) and densitometry was analyzed using software Tanonimage (V1.0).

PCR assay of specific m^{6}A-containing mRNAs

m^{6}A-containing RNAs were immunoprecipitated with anti-m^{6}A from the same amount of total RNAs of wild-type and *Hnrnpa2b1*-KO RAW264.7 cells with or without HSV-1 infection (MOI, 10). *Cgas*, *Sting*, *p204*, and *Aim2* mRNAs were assayed by qPCR. The primers were as follows: 5′-GTTCAAAGGTGTGGAGCAGC-3′ (forward) and 5′-ATTCTTTTGAATTTCACAAG-3′ (reverse) for mouse *Cgas*; 5′-GAGTGTTTACATTACACAAG-3′ (forward) and 5′-GGAGTTTATCTCCTTCCTTG-C-3′ (reverse) for *p204*; 5-GAGTGTTTACATTA-CACAAG-3′(forward) and 5′-CCTTCCTCGCAC-TTTGTTTTGC-3′ (reverse) for mouse *Aim2*; and 5′-TCAGTGGTGCAGGGAGCCGA-3′ (forward) and 5′-CGCCTGCTGGCTGTCCGTTC-3′(reverse) for mouse *Sting*.

Statistical analysis

Results are provided as means ± the standard error (SEM). All data are from at least three independent experiments performed in triplicate. Comparisons between two groups were performed using two-tailed unpaired Student's *t* test. The statistical significance of Kaplan–Meier survival curves was estimated by using the log-rank test. All statistical tests were two-sided, and significance was assigned at $P < 0.05$.

REFERENCES AND NOTES

1. T. Kawai, S. Akira, The role of pattern-recognition receptors in innate immunity: Update on Toll-like receptors. *Nat. Immunol.* **11**, 373–384 (2010). doi: 10.1038/ni.1863; pmid: 20404851
2. S. R. Paludan, A. G. Bowie, K. A. Horan, K. A. Fitzgerald, Recognition of herpesviruses by the innate immune system. *Nat. Rev. Immunol.* **11**, 143–154 (2011). doi: 10.1038/nri2937; pmid: 21267015
3. M. Marsh, A. Helenius, Virus entry: Open sesame. *Cell* **124**, 729–740 (2006). doi: 10.1016/j.cell.2006.02.007; pmid: 16497584
4. N. Kerur *et al.*, IFI16 acts as a nuclear pathogen sensor to induce the inflammasome in response to Kaposi Sarcoma-associated herpesvirus infection. *Cell Host Microbe* **9**, 363–375 (2011). doi: 10.1016/j.chom.2011.04.008; pmid: 21575908
5. M. H. Orzalli, N. A. DeLuca, D. M. Knipe, Nuclear IFI16 induction of IRF-3 signaling during herpesviral infection and degradation of IFI16 by the viral ICP0 protein. *Proc. Natl. Acad. Sci. U.S.A.* **109**, E3008–E3017 (2012). doi: 10.1073/pnas.1211302109; pmid: 23027953
6. J. Wu, Z. J. Chen, Innate immune sensing and signaling of cytosolic nucleic acids. *Annu. Rev. Immunol.* **32**, 461–488 (2014). doi: 10.1146/annurev-immunol-032713-120156; pmid: 24655297
7. Y. H. Chiu, J. B. Macmillan, Z. J. Chen, RNA polymerase III detects cytosolic DNA and induces type I interferons through the RIG-I pathway. *Cell* **138**, 576–591 (2009). doi: 10.1016/j.cell.2009.06.015; pmid: 19631370
8. B. J. Ferguson, D. S. Mansur, N. E. Peters, H. Ren, G. L. Smith, DNA-PK is a DNA sensor for IRF-3-dependent innate immunity. *eLife* **1**, e00047 (2012). doi: 10.7554/eLife.00047; pmid: 23251783
9. L. Sun, J. Wu, F. Du, X. Chen, Z. J. Chen, Cyclic GMP-AMP synthase is a cytosolic DNA sensor that activates the type I interferon pathway. *Science* **339**, 786–791 (2013). doi: 10.1126/science.1232458; pmid: 23258413
10. A. Takaoka *et al.*, DAI (DLM-1/ZBP1) is a cytosolic DNA sensor and an activator of innate immune response. *Nature* **448**, 501–505 (2007). doi: 10.1038/nature06013; pmid: 17618271
11. L. Unterholzner *et al.*, IFI16 is an innate immune sensor for intracellular DNA. *Nat. Immunol.* **11**, 997–1004 (2010). doi: 10.1038/ni.1932; pmid: 20890285
12. H. Yanai *et al.*, HMGB proteins function as universal sentinels for nucleic-acid-mediated innate immune responses. *Nature* **462**, 99–103 (2009). doi: 10.1038/nature08512; pmid: 19890330
13. P. Yang *et al.*, The cytosolic nucleic acid sensor LRRFIP1 mediates the production of type I interferon via a beta-catenin-dependent pathway. *Nat. Immunol.* **11**, 487–494 (2010). doi: 10.1038/ni.1876; pmid: 20453844
14. Z. Zhang *et al.*, The helicase DDX41 senses intracellular DNA mediated by the adaptor STING in dendritic cells. *Nat. Immunol.* **12**, 959–965 (2011). doi: 10.1038/ni.2091; pmid: 21892174
15. Y. Li *et al.*, LSm14A is a processing body-associated sensor of viral nucleic acids that initiates cellular antiviral response in the early phase of viral infection. *Proc. Natl. Acad. Sci. U.S.A.* **109**, 11770–11775 (2012). doi: 10.1073/pnas.1203405109; pmid: 22745163
16. T. Kondo *et al.*, DNA damage sensor MRE11 recognizes cytosolic double-stranded DNA and induces type I interferon by regulating STING trafficking. *Proc. Natl. Acad. Sci. U.S.A.* **110**, 2969–2974 (2013). doi: 10.1073/pnas.1222694110; pmid: 23388631
17. X. D. Li *et al.*, Pivotal roles of cGAS-cGAMP signaling in antiviral defense and immune adjuvant effects. *Science* **341**, 1390–1394 (2013). doi: 10.1126/science.1244040; pmid: 23989956
18. V. A. Rathinam *et al.*, The AIM2 inflammasome is essential for host defense against cytosolic bacteria and DNA viruses. *Nat. Immunol.* **11**, 395–402 (2010). doi: 10.1038/ni.1864; pmid: 20351692
19. S. Roth *et al.*, Rad50-CARD9 interactions link cytosolic DNA sensing to IL-1β production. *Nat. Immunol.* **15**, 538–545 (2014). doi: 10.1038/ni.2888; pmid: 24777530
20. P. Xia *et al.*, Sox2 functions as a sequence-specific DNA sensor in neutrophils to initiate innate immunity against microbial infection. *Nat. Immunol.* **16**, 366–375 (2015). doi: 10.1038/ni.3117; pmid: 25729924
21. S. P. Han, Y. H. Tang, R. Smith, Functional diversity of the hnRNPs: Past, present and perspectives. *Biochem. J.* **430**, 379–392 (2010). doi: 10.1042/BJ20100396; pmid: 20795951
22. J. Ding *et al.*, Crystal structure of the two-RRM domain of hnRNP A1 (UP1) complexed with single-stranded telomeric DNA. *Genes Dev.* **13**, 1102–1115 (1999). doi: 10.1101/gad.13.9.1102; pmid: 10323862
23. K. A. Fitzgerald *et al.*, IKKepsilon and TBK1 are essential components of the IRF3 signaling pathway. *Nat. Immunol.* **4**, 491–496 (2003). doi: 10.1038/ni921; pmid: 12692549
24. K. Honda, T. Taniguchi, IRFs: Master regulators of signalling by Toll-like receptors and cytosolic pattern-recognition receptors. *Nat. Rev. Immunol.* **6**, 644–658 (2006). doi: 10.1038/nri1900; pmid: 16932750
25. M. Yang *et al.*, E3 ubiquitin ligase CHIP facilitates Toll-like receptor signaling by recruiting and polyubiquitinating Src and atypical PKCzeta. *J. Exp. Med.* **208**, 2099–2112 (2011). doi: 10.1084/jem.20102667; pmid: 21911421
26. X. Li *et al.*, The tyrosine kinase Src promotes phosphorylation of the kinase TBK1 to facilitate type I interferon production after viral infection. *Sci. Signal.* **10**, eaae0435 (2017). doi: 10.1126/scisignal.aae0435; pmid: 28049762
27. J. D. Gary, S. Clarke, RNA and protein interactions modulated by protein arginine methylation. *Prog. Nucleic Acid Res. Mol. Biol.* **61**, 65–131 (1998). doi: 10.1016/S0079-6603(08)60825-9; pmid: 9752719
28. G. Han *et al.*, The hydroxylation activity of Jmjd6 is required for its homo-oligomerization. *J. Cell. Biochem.* **113**, 1663–1670 (2012). doi: 10.1002/jcb.24035; pmid: 22189873
29. S. S. Broyles, Vaccinia virus transcription. *J. Gen. Virol.* **84**, 2293–2303 (2003). doi: 10.1099/vir.0.18942-0; pmid: 12917449
30. J. E. Harper, S. M. Miceli, R. J. Roberts, J. L. Manley, Sequence specificity of the human mRNA N6-adenosine methylase in vitro. *Nucleic Acids Res.* **18**, 5735–5741 (1990). doi: 10.1093/nar/18.19.5735; pmid: 2216767
31. G. Jia *et al.*, N6-methyladenosine in nuclear RNA is a major substrate of the obesity-associated FTO. *Nat. Chem. Biol.* **7**, 885–887 (2011). doi: 10.1038/nchembio.687; pmid: 22002720
32. G. Zheng *et al.*, ALKBH5 is a mammalian RNA demethylase that impacts RNA metabolism and mouse fertility. *Mol. Cell* **49**, 18–29 (2013). doi: 10.1016/j.molcel.2012.10.015; pmid: 23177736
33. K. Xu *et al.*, Mettl3-mediated m^{6}A regulates spermatogonial differentiation and meiosis initiation. *Cell Res.* **27**, 1100–1114 (2017). doi: 10.1038/cr.2017.100; pmid: 28809392
34. Q. Zhang, X. Cao, Epigenetic regulation of the innate immune response to infection. *Nat. Rev. Immunol.* **19**, 417–432; Epub ahead of print (2019). doi: 10.1038/s41577-019-0151-6; pmid: 30918351
35. Q. Zheng, J. Hou, Y. Zhou, Z. Li, X. Cao, The RNA helicase DDX46 inhibits innate immunity by entrapping m^{6}A-demethylated antiviral transcripts in the nucleus. *Nat. Immunol.* **18**, 1094–1103 (2017). doi: 10.1038/ni.3830; pmid: 28846086
36. C. R. Alarcón *et al.*, HNRNPA2B1 Is a Mediator of m(6)A-Dependent Nuclear RNA Processing Events. *Cell* **162**, 1299–1308 (2015). doi: 10.1016/j.cell.2015.08.011; pmid: 26321680
37. C. Villarroya-Beltri *et al.*, Sumoylated hnRNPA2B1 controls the sorting of miRNAs into exosomes through binding to specific motifs. *Nat. Commun.* **4**, 2980 (2013). doi: 10.1038/ncomms3980; pmid: 24356509
38. H. Gordon *et al.*, Depletion of hnRNP A2/B1 overrides the nuclear retention of the HIV-1 genomic RNA. *RNA Biol.* **10**, 1714–1725 (2013). doi: 10.4161/rna.26542; pmid: 24157614
39. D. Gao *et al.*, Activation of cyclic GMP-AMP synthase by self-DNA causes autoimmune diseases. *Proc. Natl. Acad. Sci. U.S.A.* **112**, E5699–E5705 (2015). doi: 10.1073/pnas.1516465112; pmid: 26371324
40. E. E. Gray, P. M. Treuting, J. J. Woodward, D. B. Stetson, Cutting Edge: cGAS Is Required for Lethal Autoimmune Disease in the Trex1-Deficient Mouse Model of Aicardi-Goutières Syndrome. *J. Immunol.* **195**, 1939–1943 (2015). doi: 10.4049/jimmunol.1500969; pmid: 26223655
41. J. An *et al.*, Expression of Cyclic GMP-AMP Synthase in Patients With Systemic Lupus Erythematosus. *Arthritis Rheumatol.* **69**, 800–807 (2017). doi: 10.1002/art.40002; pmid: 27863149
42. V. Caneparo *et al.*, Anti-IFI16 antibodies and their relation to disease characteristics in systemic lupus erythematosus.

Lupus **22**, 607–613 (2013). doi: 10.1177/0961203313484978; pmid: 23612796
43. R. Fritsch-Stork *et al*., The spliceosomal autoantigen heterogeneous nuclear ribonucleoprotein A2 (hnRNP-A2) is a major T cell autoantigen in patients with systemic lupus erythematosus. *Arthritis Res. Ther.* **8**, R118 (2006). doi: 10.1186/ar2007; pmid: 16859514

ACKNOWLEDGMENTS

We thank Z. J. Chen (University of Texas Southwestern Medical Center) for providing *Cgas*$^{-/-}$ L929 cells and plasmids encoding *CGAS*, *STING*, and *IFI16*; G. Cheng (UCLA) for providing *Sting*$^{-/-}$ BMDMs and *Tbk1*$^{-/-}$ MEFs; T. Taniguchi (University of Tokyo) for providing *Irf3*$^{-/-}$ mice; Q. Zhou (Chinese Academy of Sciences) for providing *Mettl3*^{fl} mice; and T. Chen, W. Cun, and Y. Zhang for technical assistance. **Funding:** This work is supported by grants from the National Natural Science Foundation of China (81788101), National Key Research & Development Program of China (2018YFA0507403), and CAMS Innovation Fund for Medical Sciences (2016-12M-1-003). **Author contributions:** X.C. designed and supervised research; L.W. and M.W. performed the experiments; X.C., L.W., and M.W. analyzed data and wrote the manuscript. **Competing interests:** The authors declare no competing interests. **Data and materials availability:** The transcriptome microarray data are deposited in the NCBI Gene Expression Omnibus under accession number GSE129926. The *Hnrnpa2b1*$^{fl/fl}$ mouse strain, *Hnrnpa2b1*-KO RAW264.7 and L929 cell lines, and plasmids encoding *Jmjd6*, *Fto*, *Hnrnpa2b1*, and its mutants are available from the corresponding author on request as supplies permit, subject to a standard materials transfer agreement. All other data needed to support the conclusions of this manuscript are included in the main text and supplementary materials.

SUPPLEMENTARY MATERIALS

science.sciencemag.org/content/365/6454/eaav0758/suppl/DC1
Table S1
Figs. S1 to S13

11 August 2018; resubmitted 29 January 2019
Accepted 10 July 2019
Published online 18 July 2019
10.1126/science.aav0758

Science

Nuclear hnRNPA2B1 initiates and amplifies the innate immune response to DNA viruses

Lei Wang, Mingyue Wen and Xuetao Cao

Science **365** (6454), eaav0758.
DOI: 10.1126/science.aav0758originally published online July 18, 2019

A nuclear sensor of viral DNA?

A signaling pathway in eukaryotes known as cGAS–STING recognizes the presence of cytosolic DNA, which alerts the immune system to viral infection or cellular damage. However, the majority of DNA viruses direct their genomic DNA into nuclei, suggesting that nuclear-specific sensing is also needed. L. Wang *et al.* find that during herpes simplex virus–1 infection, heterogeneous nuclear ribonucleoprotein A2B1 forms a complex with viral DNA, homodimerizes, and is demethylated. These events result in translocation of the complex to the cytosol and activation of the immune system through type I interferon signaling. Additionally, the complex promotes N^6-methyladenosine modification and translocation of cGAS–STING–related mRNAs after DNA virus infection, further amplifying the immune response.

Science, this issue p. eaav0758